A Comprehensive Analysis Of The Antenna-Plasma Coupling Impedance For Icrh Heating In Tokamaks

Dimple Yadav [1], Vaishali Singh [1], Meenu Kaushik [2], and Vishant Gahlaut [1]
[1]Department of Physical Sciences, Banasthali Vidyapith, Rajasthan, 304022, India,
dimpleyadav1801@gmail.com, vaishalisinghchauhan8@gmail.com, vgceeri@gmail.com
[2]School of Automation, Banasthali Vidyapith, Rajasthan, 304022, India, mkceeri@gmail.com

Corresponding author : Dimple Yadav
Email: dimpleyadav1801@gmail.com

Abstract

In this article, the use of different matching techniques is reviewed, with particular emphasis on their function in antenna-plasma coupling impedance in the context of the Ion Cyclotron Resonance Heating (ICRH) technique for Tokamak systems. In magnetic confinement fusion studies, ICRH is a crucial method used to regulate and heat the plasma within a Tokamak. The performance and design of the antennas used to couple electromagnetic waves with the plasma are what determine how this heating method works. The study examines the body of research on helical antennas and evaluates their benefits, drawbacks, and difficulties. To emphasize the unique benefits provided by helical antennas in the context of the ICRH system on Tokamaks, comparisons with other antenna layouts are also explored. The study makes a significant contribution to our knowledge of helical antennas and how to optimize the antenna-plasma coupling impedance for ICRH performance by providing useful information about different impedance-matching approaches and procedures. The results might have a big impact on the creation of sophisticated Tokamak systems and help with the continuous attempts to achieve regulated and sustained nuclear fusion reactions.

Index Terms: *Helical antennas, Ion Cyclotron Resonance Heating (ICRH), Tokamak, Impedance matching techniques, Antenna-plasma coupling, Fusion reactions.*

1. INTRODUCTION

Over the decades, there has been a sharp rise in energy consumption, mirroring the population growth. Consequently, the shift towards alternative energy sources becomes a necessity. India holds the third position globally in energy consumption, trailing only China and the USA.As per the 2018 data, around 92% of the total energy consumed in India is attributed to crude oil (29.66%), coal (55.97%), and gas (6.25%), while the remaining 8% is sourced from nuclear energy, hydroelectricity, and renewable power [1].India generates about 75% of its electricity from fossil fuels, and the resulting emission of around 10.65 billion metric tons of carbon dioxide (CO_2) annually poses a severe environmental threat, contributing to the ongoing issue of global warming. Exploring environmentally sustainable energy alternatives is imperative to meet current demands. Fusion energy stands out as a promising and secure option due to its numerous advantages [2].

1.1. FUSION ENERGY

Fusion energy liberation results from the fusion process, during which two hydrogen isotopes combine to produce helium and a neutron, releasing a substantial amount of energy [1-2]. A vast quantity of heat and gravity

characterizes the core of the sun, and it is this combination that is responsible for the process of fusion. Within controlled laboratory environments, fusion reactions have been effectively accomplished using the Tokamak apparatus, which utilizes magnetic fields to confine and regulate plasma, resulting in energy production.Deuterium gas is utilized to generate the plasma, while tritium is introduced into the plasma via pellets to initiate the fusion reaction. In the sun or stars, a fusion reaction occurs at a temperature of about 10 million degrees, facilitated by high gravitational forces. Conversely, on Earth, a fusion reactor necessitates a temperature exceeding 100 million degrees Celsius, equivalent to about 10 electron volts (eV). Achieving fusion has this as one of the prerequisites. Another requirement is maintaining an adequate density of plasma particles to ensure that a majority of collisions between nuclei take place. The third requirement involves ensuring an adequate duration of plasma confinement, which presents itself as a practical challenge. The confinement of plasma is crucial to keep it at a secure distance from the reactor, thereby averting the risk of melting [3]. Figure 1 represents a basic fusion reaction of deuterium with tritium.

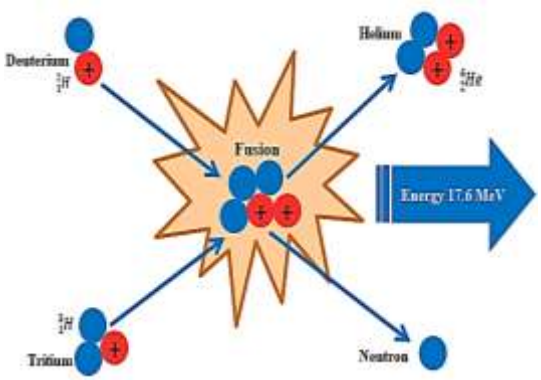

Figure 1: A basic fusion reaction of deuterium with tritium

1.2. PRODUCTION OF PLASMA AND PLASMA CONFINEMENT

The substance that forms the entirety of the universe, referred to as matter, occupies space and has mass. Existing in diverse forms like solid, liquid, and gas, matter takes on varied states. Moreover, there is another state of matter present in the universe, recognized as "the plasma state". Sir William Crookes was the first to experimentally identify the plasma state recognized as radiant matter in 1897, and the term “plasma” was coined by Irving Langmuir in 1928. The plasma state is widely acknowledged as the fourth state of matter. The ionized gas is referred to as the plasma state of matter. However, the transition from gas to plasma is not considered a thermodynamic phase transition, as it occurs gradually with rising temperature. Because of its distinctive properties that differ from fundamental states, plasma is identified as a separate state of matter, commonly recognized as the fourth state of matter. Figure 2 represents the comparison between all four states of the matter.

Similar to a gas, plasma will fill the entire volume if not confined. By employing magnetic fields, the magnetic confinement setup is tailored to confine plasma, with the inaugural selection for magnetic confinement being a linear apparatus incorporating open-field lines [4]. The formation of a torus structure, called Tokamak, occurred as a response to losses in the linear device, incorporating both toroidal and poloidal fields [3-5]. The Tokamak principle, pioneered by a Soviet physicist, remains one of the most effective designs for generating fusion power to this day. Figure 2 represents the conceptual depiction of matter transitioning into plasma.

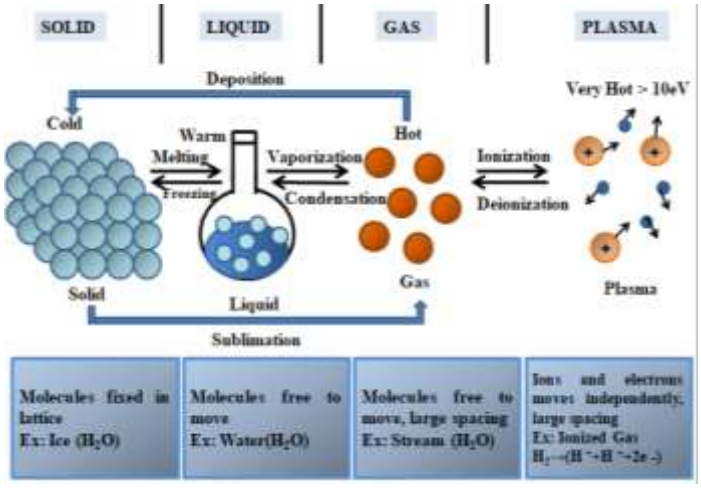

Figure 2: A conceptual depiction of matter transitioning into plasma has been illustrated.

1.3. TOKAMAK

Tokamak is a Russian word meaning large magnetic bottle. It is a device that is used to study plasma state and property. Figure 3 represents the basic diagram of tokamak.

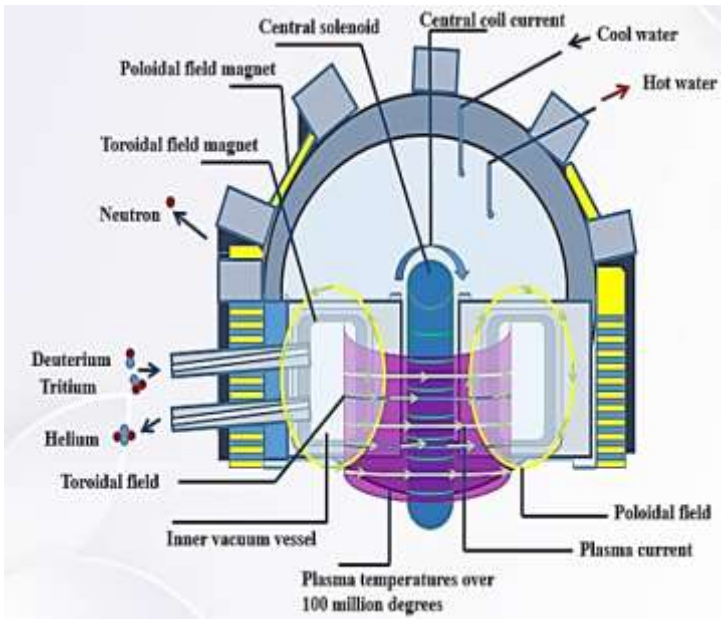

Figure 3: Tokamak- A Promising Technology for Nuclear Fusion

1.3.1. BACKGROUND

The tokamak functions as a magnetic containment device, utilized to regulate and confine high-temperature plasma, facilitating controlled fusion reactions for potential energy production [4]. Massive amounts of energy are released during the fusion process between atoms, and the exterior walls of the device collect this energy through heat. The generated heat will produce steam in the fusion power plant, which will then be converted to electricity through the use of turbines or generators.

Due to scattering, there is an energy loss, preventing the fusion process. In 1944, Enrico Fermi calculated that to maintain the fusion reaction, a self-sustaining temperature of around 50,000,000K is necessary. In the year 1945, George Paget, a British scientist, undertook several unsuccessful initiatives to develop a feasible fusion apparatus built upon the pinch effect, a method that showed potential. In the beginning, Russian physicists Sakharov and Tamm recommended refraining from the use of external magnets, as the plasma's current strength is adequate for confinement major proponents for the static toroidal setup, Golovin as well as Natan Yavlinsky, noted notable instability, such as sausage and kink instabilities, in the linear pinch notion [4]. The ‘stabilized pinch' presents a further approach by creating a field outside the chamber with additional magnets before the plasma discharge. Sakharov proposed a novel approach to steady the plasma by lowering the current and employing strong outer magnets for plasma confinement. Table 1 shows a review of different tokamaks across the globe.

Table 1: An overview of well-known experimental reactors across the globe

Tokamak	**Power**	**Frequency range**	**Reference**
Aditya	200kW	20-47 MHz	5
SST-1	1.5MW	22.8-92 MHz	6-14
Alcator C-Mod	~6MW	40-80 MHz	15-22
ASDEX upgrade	6MW	30-120 MHz	23-27
JET	36MW	25-55 MHz	28-34
WEST	16MW	40-80 MHz	35-37
ITER	20MW/ Antenna	40-55 MHz	38-49

The first Tokamak, T-1, became operational in 1958 and exhibited notable energy losses due to impurities present in the plasma in search of a solution, the T-2 miniature device was created. The outcomes cleared the path for the development of Tokamaks around the world, including "The Culham Five" around the end of 1968, T-3, T-4, and TM-2 in 1968. Many nations began working on Tokamak development in the middle of the 1970s and by the end of the decade, several results suggested that fusion might be achieved practically—just not through a single reactor. The magnetic compression concept was put forth by Princeton Plasma Physics Laboratory (PPPL), while Oak Ridge Laboratory proposed the use of neutral beam injection. The findings from Princeton Large Torus (PLT) regarding beamforming heating lay the groundwork for a forthcoming fusion reactor. In 1979, the T-7 Tokamak achieved success with the utilization of superconducting magnets. Subsequently, other Tokamaks such as T-15, Alcator C-

mod [15-22], JT-60 [25], JET [28-34], TFTR [35], TEXTOR [37], and others followed suit. Initiated efforts on ICRH heating and conducted experimentsusing deuterium and tritium as fuel, revealing new challenges that constrain performance. In 1986, the USA, Japan, and the Soviet Union signed an agreement to collaborate on the construction of a larger and more potent apparatus, targeting a q factor of approximately 10. The International Thermonuclear Experimental Reactor (ITER) Association was founded as a result of this cooperative Endeavour [4]. In 2005, India formally became a part of the ITER project.

1.3.2. PLASMA HEATING

The temperature of the plasma inside the vessel is a crucial factor in the context of fusion. To facilitate a fusion reaction within the Tokamak, the plasma temperature must be sustained at around one hundred million degrees Celsius [2-3]. Attaining such elevated temperatures poses a primary challenge for scientists. Plasma is extremely responsive to electromagnetic waves and electrically conductive due to its ionized gas state. A transformer coil positioned around the vessel is used to induce a current to initiate the very first phase of plasma heating. It is also known as ohmic heating, and it works similarly to the way a heating device heats up. The quantity of heat produced inside the Tokamak is contingent on the level of electric current flowing and the plasma's resistance. Ohmic heating loses its effectiveness as the plasma temperature rises, leading to a reduction in resistance. Temperatures ranging from twenty to thirty million degrees Celsius can be reached with this heating technique. It is necessary to use a variety of heating techniques, including magnetic compression, neutral beam injection (NBI), ECRH (Electron Cyclotron Resonance Heating), ICRH, and others, to reach the optimal temperature for starting fusion [5–30]. Figure 4 Shows the schematic view of the plasma heating.

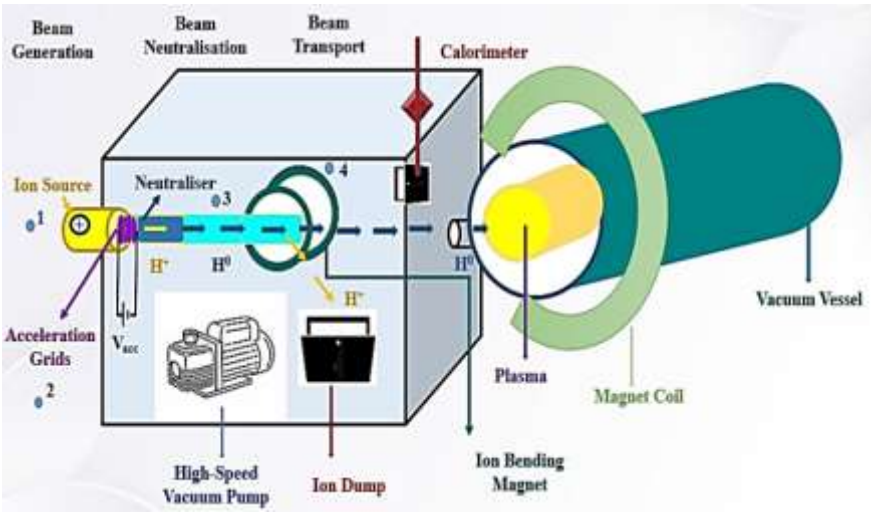

Figure 4: Schematic Diagram of Plasma Heating

- **Neutral Beam Injection (NBI)**

The high-power photon of neutral particles is introduced into the plasma via the NBI method.The plasma receives energy through coulomb interactions with the particles. The concept of NBI was initially put forth by Oak Ridge Laboratory in the mid-1970s [4, 15]. The location of ITER's initial operating NBI facility is near Padova. Although plasma heating is its primary usage, this technology is also employed in feedback management via the employment of a pulsed beam in addition to a diagnostic tool.

- **Magnetic Compression**

It is a method wherein the plasma undergoes compression through the enhancement of magnetic field confinement. The ions are compressed together, bringing them closer to one another and creating the requisite plasma density for the fusion reaction. The heating method has been utilized in the initial stages of fusion exploration. The concept of magnetic compression is still vital to the overall fusion design even though it is no longer in use.

- **Ion Cyclotron Resonance Heating (ICRH)**

Throughout recent decades, there have been continuous endeavors to explore how electromagnetic waves interact with plasma. Various fusion devices, including stellarators [15], mirror machines [4], as well as Tokamak [4-50], use the process of plasma heating via electromagnetic waves. Transmitting electromagnetic wave energy with a high frequency to the plasma is the process of Radio Frequency (RF) heating. Using RF oscillators as well as generators, the electromagnetic waves originate externally to the vessel. A rise in the motion energy of ions is the outcome result of the resonant interaction in the middle of such electromagnetic waves as well as the ionized gas. The power is subsequently passed on to other particles within the plasma through collisions, leading to the occurrence of heating.

- **Electron cyclotron resonance heating (ECRH)**

To raise the plasma temperature for fusion levels, ECRH utilizes microwave energy absorbed at frequencies corresponding to the resonance of electrons. When the incoming wave frequency aligns with that of electrons in a magnetic environment, this phenomenon occurs [15, 27]. Within the Tokamak, the frequency of the ECRH system can vary between 28 and 170 GHz, generated by specific free-electron lasers as well as gyrotron tubes.

1.3.3. OVERVIEW OF ICRH SYSTEM

India plays a pivotal role in the ITER Tokamak project, overseeing the supply of ECRH and ICRH heating systems, power supplies, and various other obligations. Within the Tokamak, the plasma is elevated to temperatures ranging in the scores of millions of degrees Celsius to attain the necessary fusion reaction rate. Employing the ICRH system for heating Tokamak plasma emerges as a promising method, particularly notable for its effectiveness in low densities as well as low magnetic fields. Moreover, the technology employed in the generation and transmission of high-power RF is comparatively cost-effective. As cited in reference [6], the ICRH setups include an RF generator, transmission conduits, a sensing unit, a tuning system, and RF antennas. The ICRH antenna receives up to megawatts of radiofrequency power to transmit power to the source via the antenna. These RF antennae then contribute to the overall plasma heating towards the fusion process by emitting radiofrequency waves within the tokamak at the plasma's ICRF frequency. Antenna impedance changes as a result of dynamic fluctuations in the plasma state around radiofrequency antennas [6-14], [38-41]. A variety of studies have provided detailed insights into the ICRH system. Below is a detailed explanation of the studies that have been carried out worldwide on the Tokamak ICRH system. These studies cover the system's structure, operating frequency range, different matching networks, detecting units, and issues that have been identified.

After the introduction, the structure of this paper involves nine sections. In section 2, an overview of the ICRH system’s structure and RF transmission system on SST-1 is elaborated. Section 3 represents the review of relevant previous works. Section 4 shows the VSWR curve formulation. Non-linear least square techniques are discussed in section 5. Section 6 presents the state-of-the-art. Section 7 focuses on the conclusion. Section 8 shows the list of abbreviations.

2. AN OVERVIEW OF THE ICRH SYSTEM'S STRUCTURE AND RF TRANSMISSION SYSTEM ON SST-1

A detecting unit, tuning component, response mechanism, radiofrequency transmitter, potent radio frequency generators, and extended transmission lines comprise the basic architecture of the ICRH apparatus employed in each Tokamak [5-53]. Figure 5 represents the block diagram of ICRH heating on an SST-1.

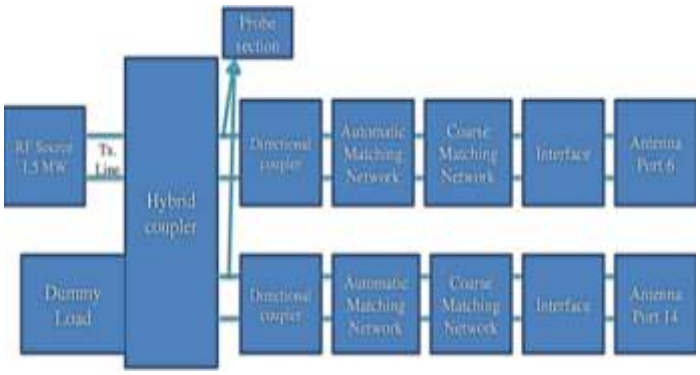

Figure 5: Block Diagram of ICRH Heating on a SST-1

On SST-1 [6], the ICRH system operates using a 1.5MW generator. Meanwhile, ITER [47] has proposed the coupling of 20MW of power to the ICRH antenna. The Aditya Tokamak utilizes a 9-inch coaxial Transmission Line (TL) with a length of approximately 53 meters, while the SST-1 employs a 100-meter-long TL [6, 9]. Below Figure 6 represents a brief description of the architecture of the ICRH system and Figure 7 shows the RF transmission system on SST-1.

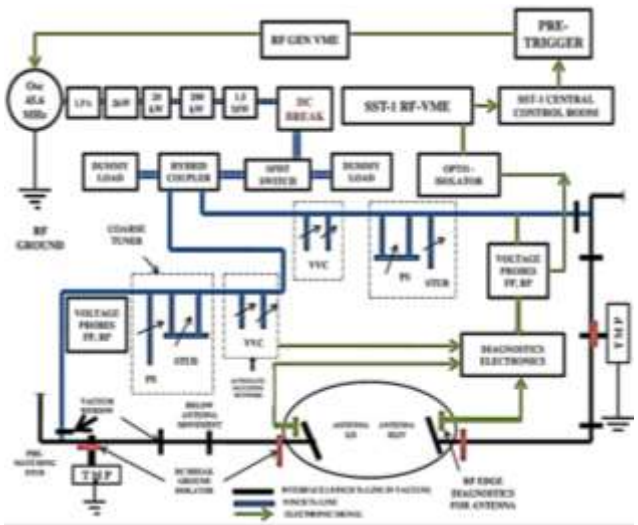

Figure 6: The Brief architecture of the ICRH system on SST-1

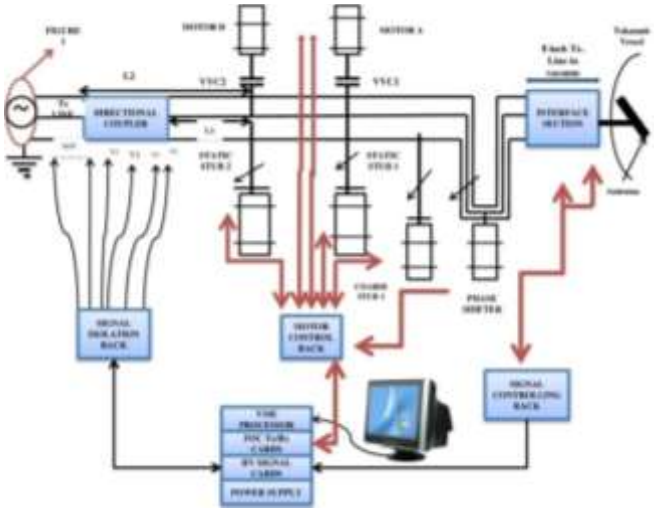

Figure 7: RF Transmission system on SST-1

2.1. Advances in Antenna-Plasma Coupling Techniques

Dynamic changes in plasma properties occur in front of RF antennae, leading to corresponding variations in antenna impedance. It is difficult to match and manage fluctuations in antenna impedance on a few millisecond time scales. Every Tokamak ICRH system has a matching system and a detecting unit to protect the system and guarantee the best possible supply of input power through the ionized gas. Figure 8shows the diagrammatic representation of antenna-plasma coupling impedance.

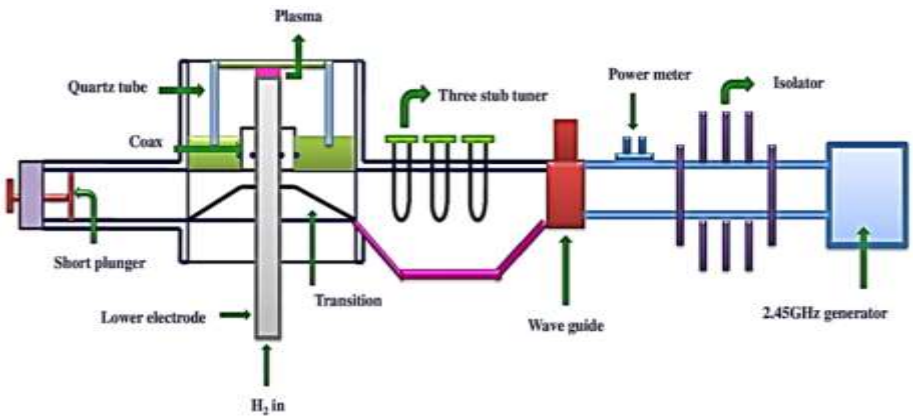

Figure 8: Diagrammatic representation of Antenna-Plasma Coupling Impedance

This section's discussion dives into a thorough examination of the matching, feedback, and detecting systems that are used in various Tokamak designs as shown in Table 2.

Table 2: Review of matching techniques used in different tokamaks

S. No.	Tokamak	Heating Method	Matching Techniques	Findings	Reference
1.	SST-1	ICRF heating	i. 3dB hybrid coupler ii. Stub tuner iii. Phase shifter	i. The power distribution for driving both antennas is achieved through the use of a 3dB hybrid coupler. ii. The VME-based data acquisition system, specifically the VERSA-Module Euro card, is integral to real-time control in the SST-1 system.	Bora et al., [6]
2.	SST-1, ITER	ICRH heating	i. 3dB hybrid coupler ii. Stub tuner iii. Phase shifter	i. Designed a 3dB hybrid coupler using strip-line technology. ii. Investigates the impact of junction disparity in high-energy settings and delves into the augmentation of frequency range through the utilization of multi-section coupled lines.	Yadav et al., [54-56]
3.	SST-1	ICRH heating	i. Stub tuner ii. Phase shifter	i. Within a brief timeframe, offline matching is executed, whereas online matching is completed in roughly 120 milliseconds.	Joshi et al., [9]
4.	JET and ASDEX	ICRH heating	i. Hybrid coupler ii. Stub tuner	i. Responding to impedance variations within a short period, the matching components exhibit different speeds, with the stub at 5 cm/sec and the trombone at 16.5 cm/sec. In JT-60 U, the trombone moves at 0.5 cm/sec, and the stub at 2 cm/sec.	Noterdaeme et al., [25]
5.	ITER	ICRH heating	i. Four hybrid couplers ii. CT junctions iii. De-coupler iv. Feedback-controlled stub	i. The modeling-derived load durability capability and antenna frequency range exhibit a striking similarity to the outcomes of the TOPICA simulation, a correspondence that holds for the ITER setup. ii. Growing the prototype dimensions to fivefold that of ITER's ICRH which involves augmenting the frequency and reducing the dimensions to one-fifth of the actual system. This alteration is implemented to examine and manage the effects of mutual interaction and fluctuations in loading.	Messiaen et al., [42]
6.	ITER	ICRH heating	i. De-coupler ii. Stub tuner iii. Phase shifters	i. Discussed the development of an algorithm utilizing an error function, accounting for both real and imaginary	Grine et al., [47]

				aspects, enabling real-time matching of impedance variations.	
7.	Alcator C-Mod	ICRH heating	i. Liquid phase shifter ii. Stub tuner	i. Stubs maintain a response time within the range of seconds, suggesting a slow operational pace.	Kumazawa et al., [55]
8.	Alcator C-Mod	ICRF system	i. Fast ferrite tuner ii. Triple stub tuner	i. Effectively match variations in real-time; nevertheless, the major drawback of the ferrite tuner lies in the pronounced RF losses resulting from biasing.	Lin et al., [19]
9.	ITER	ICRF system	i. Single Stub ii. Double stub iii. Pre-matching element iv. Faraday screen	i. A single triplet strap is employed for optimization, and the design is structured around scaled frequency parameters. ii. The antenna is accompanied by the service stub, resulting in amplified coupled power and a broadband frequency response.	P. Dumortier et al., [43]

3. REVIEW OF RELEVANT PREVIOUS WORKS

Numerous studies have been carried out on plasma within the presence of non-uniform magnetic fields in astrophysical and laboratory plasmas [18, 20]. Forinstance, magnetic reconnection is one of the well-known astrophysical phenomena caused by plasma flow along a non-uniform magnetic field [50]. A study of various techniques used for antenna-plasma coupling is shown in Table 3.

Table 3: A study of various techniques and outcomes is given below:

S.no.	**Cited by**	**Favored Matching Techniques**	**Outcomes**	**Reference No.**
1.	J. Staples et al.	Capacitive voltage dividers	1. Dual frequency operation has been successfully generated to get the cleanest source operation.	56.
2.	Qin Chengming et al.	Stub tuner	1. It isexamined that traditional stub tuning was inferior compared to a liquid-based stub tuning method. 2. Due to the many advantageous aspects of liquid stub tuners, this has been proven to be very useful in ICRF heating experiments.	57.
3.	Pan Yaping et al.	Liquid stub tuner	1. An efficient method was used to solve the circumfluence problem. 2. The delay time is contingent upon the electromotive actuator's response time.	58.

4.	A. Girard et al.	ECR source	1. An attempt has been made for the understanding of ECRIS plasma. 2. Significant development has been attained in both the field of physics and technology through multi-charged beams.	59.
5.	D. Bora et al.	ICRH system	1. The antenna impedance matching has been successfully conducted using stubs and phase shifters. 2. In the matching unit and antenna system, twenty voltage probes are being placed where VSWR is quite high.	60.
6.	K.Saito et al.	Trial-and-error method	1. The prediction was made to optimize the fluid levels and manifested the low input power of the reflection coefficient using the feedback control-based method. 2. Furthermore, there is a reduction of reflected power, and using liquid stub tuners, makes impedance matching useful for future fusion reactors.	61.
7.	D. Bora et al.	Inductively coupled plasma chamber	1. On SST-1, the ICRF system has been installed, and thorough testing has validated the functionality of all its components. 2. The launcher was thoroughly prepared for fusion on the SST-1 machine and verified for UHV compatibility.	62.
8.	Giorgio Bacelli et al.	Double sub fast ferrite tuning system	1. In terms of convergence, the Hierarchical controller showed good performance. 2. A multivariable controller has also been fabricated that observes the dependence of Im[ZPL] on both CL and CT.	63.
9.	Y.Lin et al.	Triple stub fast ferrite tuning system	1. On the ICRF antenna, there has been a successful implementation of a triple stub real-time FFT system. 2. The result has shown a power reflection of about 1 % in a considerable number of plasma parameters.	64.
10.	R. Harmsworth et al.	Neutral Beam(NB) injector	1. The revamped setup of the ITER beam neutralization system offers notable benefits. 2. For further computation in the adverse ion accelerator, a choice has been made in the favor of MAMuG accelerator concept, and later on, a detailed design has been verified.	65.
11.	Raj Singh et al.	Conventional phase shifters and liquid phase shifters	1. Liquid phase shifter played an important role in the Aditya tokamak. 2. At present, one phase shifter and one stub tuner are connected in Aditya Tokamak. 3. Furthermore, now two phase shifters and two stub tuners are being upgraded due to the impedance-matching network	66.
12.	Sunil Dani et al.	Multi-limb phase shifter	1. The designed parameter has been tested on this system and was also used by a fast ferrite tuner for testing the 100 kW power at the frequency range of 91.2 MHz.	67.

13.	Dharmendra Rathi et al.	Automatic ICRH vacuum system	1. Schematics of automated vacuum systems have been established successfully in the context of raising the temperature.	68.
14.	Kishore Mishra et al.	Fast wave electron heating	1. Established the direct electron heating on tokamak Aditya with the rise in temperature of an electron with radio frequency power. 2. Significant plasma density rise has been observed due to the low impurity production.	69.
15.	H. Faugel et al.	Double stud tuners and directional coupler	1. Good measurement has been observed by installing the electricity detectors in the antenna experiencing disruptions due to the brief circuits. 2. For the cooling of the coaxial transmission line, components, and antenna are necessary for the long pulse ICRF system.	70.
16.	Gaurab Bansal et al.	Single driver negative ion source	1. An experiment has been performed on the ROBIN to test the RF-based single-driven negative ion source. 2. The extraction system has been commissioned and installation of the system is being initiated. 3. The frequency stability of the type of ferrite that is used in the matching network is still an issue.	71.
17.	Y. Lin et al.	Real-time fast ferrite tuning system	1. On the Alcator-C-mod, the plasma impedance matching has been experienced on the two traditional ports using ferrite tuners. 2. The system has attained impedance matching with the reflected power of less than 1%.	72.
18.	Raj Singh et al.	Liquid Stub Tuner	1. This study presents a novel 1–5/8” liquid stub tuner (LST) specifically designed to achieve efficient impedance matching for ion cyclotron RF signal transmission. 2. The primary aim is to enhance power transmission efficiency from the RF source to the antenna in Steady-State Superconducting and Aditya Tokamaks.	73.
19.	Dimple Yadav et al.	Automatic matching design at the center	1. An approach for designing a two-arm resistively loaded spiral antenna, as per the port constraints of SST-1 tokamak has been presented. 2. Using this technique, it becomes possible to launch electron cyclotron resonance (ECR) waves at the second harmonics with a magnetic field of 0.75T at the frequency of 284MHz.	74.

4. VSWR CURVE FORMULATION

4.1. INTRODUCTION TO PROBLEM:

ICRH has been recognized as a promising method for elevating plasma temperatures. Nevertheless, a significant challenge in ICRH lies in the coupling of RF power to the plasma.As a result of its ionized state, plasma exhibits extremely minimal resistive impedance. Therefore, ensuring alignment between the RF source impedance and the plasma impedance is imperative for ICRF heating. To achieve conformity with the plasma impedance, it is essential to first ascertain its value.In traditional approaches, the plasma impedance is determined through the utilization of the VSWR curve technique. In Aditya and SST-1, akin to tokamak devices, plasma endures for several hundred milliseconds, while the RF power supplied to the plasma amounts to a few hundred kilowatts.Within such a brief duration and with such elevated power levels, determining the VSWR curve using the sliding probe method becomes unfeasible. Therefore, the fixed probe technique is employed to ascertain plasma impedance.The voltage signal captured by the probe from the transmission line is analyzed to determine both the amplitude and phase of the reflection coefficient, thereby reducing the plasma impedance.The voltage measurements from the probe are transmitted across a distance of approximately 50 meters.Throughout this procedure, inaccuracies are introduced into the probe data.To mitigate this error, the least squares method has been applied to the voltage probe data.Additionally, under typical circumstances, a set of approximately 15 probes is employed along a span equivalent to λ/2 to ascertain the VSWR curve [75]. In this paper, a comprehensive review is provided concerning the optimal curve fitting technique aimed at reducing errors in determining both the magnitude and phase of the reflection coefficient, consequently unveiling the plasma impedance observed by the antenna.

4.2. VOLTAGE STANDING WAVE CURVE DERIVATION

The voltage distribution in a uniform two-wire transmission line under single-frequency time harmonic condition is expressed as

$$V(Z) = V_1 e^{-\gamma z} + V_2 e^{+\gamma z} \quad (1.1)$$

Where V_1 and V_2 are the random phasor voltages, as well as $\gamma=\alpha+j\beta$,is the wave constant. The equation of the current distribution on the line is given by

$$I(Z) + \frac{1}{Z_0}(V_1 e^{-\gamma Z} - V_2 e^{+\gamma Z}) \quad (1.2)$$

The transmission circuit is shown below in Figure 9.

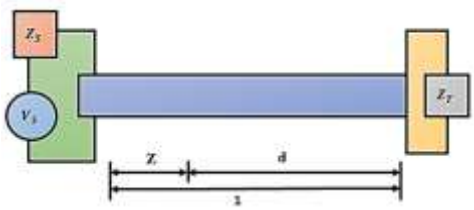

Figure 9: RF Power Flow

In this context, 1 stands for the complete length from the source to the load, with d indicating the distance from the load to a specific location along the transmission line.

The reflection coefficient at the terminal load termination is specified by

$$\rho_T = \frac{V_2 e^{+\gamma l}}{V_1 e^{-\gamma l}} = \frac{\frac{Z_r}{Z_0}-1}{\frac{Z_T}{Z_0}+1} \quad (1.3)$$

The equations (1.1) and (1.2) can be rewritten using $Z = l - d$

$$V(d) = V_1 e^{-\gamma(l-d)} + V_2 e^{+\gamma(l-d)} \quad (1.4)$$

$$V(d) = V_1 e^{-\gamma l+\gamma d} + V_2 e^{\gamma l-\gamma d} \quad (1.5)$$

$$V(d) = V_1 e^{-\gamma l}(e^{\gamma d} + \frac{V_2 e^{\gamma l}}{V_1 e^{\gamma l}} e^{-\gamma d}) \quad (1.6)$$

$$V(d) = V_1 e^{-\gamma l}(e^{\gamma d} + \rho_T e^{-\gamma d}) \quad (1.7)$$

As ρ_T is a complex value and can written in terms of magnitude of reflection coefficient and phase as shown below in equation 1.8.

$$\rho_T = |\rho_T| e^{j\emptyset_T} = e^{-2(p+jq)} \quad (1.8)$$

Where,

$$|\rho_T| = e^{-2p} \quad (1.9)$$

$$e^{2p} = \frac{1}{|\rho_T|} \quad (1.10)$$

$$p = ln \frac{1}{\sqrt{|\rho_T|}} \quad (1.11)$$

ρ_T is the magnitude part and will vary from 0 to 1. Whenρ_T is 1 the value of p is 0 and when ρ_T is 0 or considering the value as 0.001 the value obtained of p is approximately 4in equation no. 1.11.

$$\emptyset_T = -2q \quad (1.12)$$

$$q = -\frac{1}{2}\emptyset_T \quad (1.13)$$

The value of $\emptyset_T$ varies from –π to π in equation 1.12 and hence q will vary from –π/2 to +π/2 in equation 1.13.

$|\rho_T| e^{j\emptyset_T} = e^{-2(p+jq)}$ in equation 1.8, this assumption is done to simplify the VSWR equation which can be shown below

Putting this value of ρ_T into (1.7)

$$V(d) = V_1 e^{-\gamma l}(e^{\gamma d} + e^{-2(p+jq)} e^{-\gamma d}) \quad (1.14)$$

$$V(d) = V_1 e^{-\gamma l} e^{-(p+jq)}\left(e^{(p+jq)} e^{\gamma d} + e^{-(p+jq)} e^{-\gamma d}\right) \quad (1.15)$$

Putting $e^{-(p+jq)} = \sqrt{\rho_T}$ in equation 1.15 we get,

$$V(d) = V_1 e^{-\gamma l}\sqrt{\rho_T}(e^{(p+jq)} e^{\gamma d} + e^{-(p+jq)} e^{-\gamma d}) \quad (1.16)$$

Putting the value $\gamma = \alpha + j\beta$ in equation 1.16

$$V(d) = V_1 e^{-\gamma l}\sqrt{\rho_T}(e^{(p+jq)}e^{(\alpha+j\beta)d} + e^{-(p+jq)}e^{-(\alpha+j\beta)d} \quad (1.17)$$

$$V(d) = V_1 e^{-\gamma l}\sqrt{\rho_T}\{e^{(\alpha d+p)+j(\beta d+q)} + e^{-(\alpha d+p)-j(\beta d+q)}\} \quad (1.18)$$

$$V(d) = 2V_1 e^{-\gamma l}\sqrt{\rho_T}cosh\{(\alpha d + p) + j(\beta d + q)\} \quad (1.19)$$

$$V(d) = 2V_1 e^{-\gamma l}\sqrt{\rho_T}[cosh(\alpha d + p)\, cosh(j(\beta d + q)) + sinh(\alpha d + p)\, sinh\,(j(\beta d + q))] \quad (1.20)$$

$(where\ cosh(x + jy) = coash\ x\ cos(jy) + sinh\ x\ sih(jy))$, putting this in equation 1.20, we obtain

$$V(d) = 2V_1 e^{-\gamma l}\sqrt{\rho_T}[cosh(\alpha d + p)\, cos(\beta d + q) + j\ sinh\,(\alpha d + p) sin\,(\beta d + q)] \quad (1.21)$$

$(where\ cosh(jy) = cos\ x\ and\ sinh(jy) = j\ sin\ y)$

Finding the magnitude of the standing wave in equation 1.21

$$|V(d)| = \left|2V_1 e^{-\gamma l}\sqrt{\rho_T}\right|\left\{\{cosh^2(\alpha d + p)cos^2(\beta d + q) + sinh^2(\alpha d + p)sin^2(\beta d + q)\}^{\frac{1}{2}}\right\} \quad (1.22)$$

$$= \left|2V_1 e^{-\gamma l}\sqrt{\rho_T}\right|\left\{\{(1 + sinh^2(\alpha d + p))cos^2(\beta d + q) + sinh^2(\alpha d + p)sin^2(\beta d + q)\}^{\frac{1}{2}}\right\} \quad (1.23)$$

$$= \left|2V_1 e^{-\gamma l}\sqrt{\rho_T}\right|\left\{\{(cos^2(\alpha d + p)) + sinh^2(\alpha d + p)cos^2(\beta d + q) + sinh^2(\alpha d + p)sin^2(\beta d + q)\}^{\frac{1}{2}}\right\} \quad (1.24)$$

$$= \left|2V_1 e^{-\gamma l}\sqrt{\rho_T}\right|\left\{\left(cos^2(\beta d + q) + sinh^2(\alpha d + p)^{\frac{1}{2}}\right)\right\} \quad (1.25)$$

And

$$\xi(d) = tan^{-1}\{(tanh(\alpha d + p) + tan\,(\beta d + q)\} \quad (1.26)$$

Where $\xi(d)$is the phase variation of the standing wave in equation 1.26.

The scaling factor $\left|2V_1 e^{-\gamma l}\sqrt{\rho_T}\right|$ is the magnitude term in equation 1.25 and can be assumed as constant. So making $\left|2V_1 e^{-\gamma l}\sqrt{\rho_T}\right|\ as'a', we\ get$,

$$|V(d)| = a^*\left\{\{sinh^2(\alpha d + p) + cos^2(\beta d + q)\}^{\frac{1}{2}}\right\} \quad (1.27)$$

For a no-loss less $\alpha = 0$; so

$$|V(d)| = a^*\left\{\{sinh^2(p) + cos^2(\beta d + q)\}^{\frac{1}{2}}\right\} \quad (1.28)$$

No presumption has been taken into account in deriving this equation, thus providing VSWR curve values for various distances (d) from the terminal load[75]. In the ICRF heating experiment, frequency is of the order of a few tens of MHz and power is about 1-2 MW. In such a situation probes are fixed at certain intervals on the coaxial transmission line and voltage samples are obtained using these probes. These voltage samples are used to draw the voltage standing wave curve. There may be a possibility that these voltage samples may have errors. The source of

error may be non-uniform penetration of the probes into the transmission line. Due to unequal penetration, the voltage picked up by the probes may not be proportional to the voltage available at that point. The second source of error may be unequal attenuation of the cables used to transport the signals from voltage probes to the data acquisition rack. The third source of error may be the detectors. Detectors are used to convert RF to DC. These detectors may not give the equal value of DC for the equal value of RF power and hence introduce the error. These errors require some technique to fit a curve with minimum error with voltage probe data. In actuality, we will have voltage sample points at some fixed distance. So we need to find the parameter a, p, q that fits to discrete curve with minimum error squared. The voltage picked up by the probe is a nonlinear function of p and q, so the non-linear least square technique will be used.

5. NON-LINEAR LEAST SQUARE TECHNIQUE

The non-linear least squares methodology is a form of least squares analysis employed to match a collection of m observations with a model featuring non-linearity in n unspecified parameters (where m is greater than n) [75].It finds utility in certain varieties of non-linear regression analysis. The fundamental principle of this approachis to estimate the model using a linear approximation and then refine the parameters through successive iterations. Numerous resemblances exist with linear least squares, yet there are also notable distinctions.

In the realm of mathematics and computing, the Levenberg-Marquardt algorithm (LMA), alternatively recognized as the damped least-squares (DLS)technique, furnishes a computational resolution to the task of minimizing a function, typically non-linear across a parameter space of the function. These minimization challenges emerge predominantly in curve fitting using least squares, where the function's dependency on the parameters is non-linear

The LMA bridges the gap between the Gauss-Newton algorithm (GNA) and the gradient descent approach. The LMA demonstrates greater resilience compared to the GNA, indicating its ability to often reach a solution even when initiated from a considerable distance away from the eventual minimum. In cases where functions behave predictability and initial parameters are sensible, the LMA typically exhibits a slightly slower pace compared to the GNA

5.1. THEORY OF GAUSS-NEWTON METHOD

The main utilization of the Levenberg-Marquardt algorithm lies in addressing the least squares curve fitting quandary, involving a collection of m observed data pairs consisting of independent and dependent variables, (xi, yi), enhancing the parameters β (where β is the set of parameters) of the model curve f(x, β) such that the total of the squares of the deviationsbecomes minimal.

$$F(\beta) = \sum_{i=1}^{m}[y_i - f(x_i, \beta)]^2 \quad (1.29)$$

The Gauss-Newton technique is an algorithm utilized to minimize the sum of the squares of the discrepancies between the data as well as the non-linear equation.The fundamental principle driving the method is the utilization of a Taylor series expansion to represent the original non-linear equation in an approximate linear format.Subsequently, the least squares method can be employed to derive fresh estimations of the parameters, aiming to diminish the residual or error.To demonstrate the procedure, initially, the association between the non-linear equation and the data can be broadly articulated as

$$y_i = f(x_i; a_0; a_1 \dots\dots\dots a_n) \quad (1.30)$$

Where y_i = a recorded value of the outcome variable as shown in equation 1.29, $f(x_i; a_0; a_1 \dots \dots \dots . a_n)$ is a result of the independent variable x_i and nonlinear relationship of the variables$a_0, a_1 \dots \dots \dots . a_n$. For convenience, this model can be condensed by excluding the variables as

$$y_i = f(x_i, \beta) \quad (1.31)$$

Where β= $[a_0, a_1 \dots \dots \dots . a_n]$

Taylor series in one dimension is represented in equation 1.31

$$f(x_0 + \Delta x) = f(x_0) + \Delta x f'(x_0) + \frac{1}{2!}(\Delta x)^2 f^{"}(x_0 + \cdots) \quad (1.32)$$

The non-linear model can be elucidated using the Taylor series centered on the parameter values and truncated after the initial derivative. For instance, in a scenario involving two parameters,

$$f(x_i, \beta + \delta) \approx f(x_i, \beta) + \frac{\partial f(x_i,\beta)}{\partial a_0}\Delta a_0 + \frac{\partial f(x_i,\beta)}{\partial a_1}\Delta a_1 \quad (1.33)$$

$$f(x_i, \beta + \delta) \approx f\left(x_{i,}\beta\right) + J_i\delta \quad (1.34)$$

Where,

$J_i = \frac{\partial f(x_i)}{\partial \beta}$ is a gradient (row vector) of $f$concerning β as written in equation 1.33

At the lowest point of the sum of squares $F(\beta)$, the gradient of F to δ will be zero. The preceding primary estimation of $f(x_i, \beta + \delta)$ gives

$$F(\beta + \delta) \approx \sum_{i=1}^{m}(y_i - f\left(x_{i,}\beta\right) - J_i\delta)^2 \quad (1.35)$$

Or in vector notation,

$$F(\beta + \delta) \approx \|y - f(x, \beta) - J\beta\|^2 \quad (1.36)$$

Let's assume$y_i - f(x_i, \beta)$ in the above equation 1.35 to be $Y_i$for simplicity.

$$F(\beta + \delta) \approx \|Y - J\delta\|^2 \quad (1.37)$$

$$F \approx \|Y - J\delta\|^2 \quad (1.38)$$

$$F \approx (Y - J\delta)^T(Y - J\delta) \quad (1.39)$$

$$F \approx (Y^T - J^T\delta^T)(Y - J\delta) \quad (1.40)$$

$$F \approx Y^TY - Y^TJ\delta - \delta^TJ^TY + \delta^TJ^TJ\delta \quad (1.41)$$

$$F \approx Y^TY - 2\delta^TJ^TY + \delta^TJ^TJ\delta \quad (1.42)$$

Computing the gradient of the above equation (1.41) concerning to δ we get,

$$\frac{\partial F}{\partial \delta} = \frac{\partial}{\partial \delta}(Y^TY - 2\delta^TJ^TY + \delta^TT^TJ\delta) \quad (1.43)$$

$$\frac{\partial F}{\partial \delta} = -2J^T Y + 2J^T J\delta \quad (1.44)$$

Establishing the outcome as zero yields

$$0 = -2J^T Y + 2J^T J\delta \quad (1.45)$$

$$(J^T J)\delta = J^T Y$$

By solving above equation 1.44 we get,

$$(J^T J)\delta = J^T (y_i - f(x_i, \beta)) \quad (1.46)$$

$$\delta = (J^T J)^{-1} J^T (y_i - f(x_i, \beta)) \quad (1.47)$$

Here, J denotes the Jacobian matrix where each i^{th}rowis equivalent to J_i, while f and y represent the vectors containing the i^{th} component $f(x_i, \beta)$ and y_i, respectively.

Initially, the random guess is chosen as β. After that the value is calculated by solving the equation (1.3) and then the new value of the parameter is updated as $+\delta$. This equation is iterated till the value of δ is reached to the acceptable value. This algorithm is known as the Gauss-Newton Method.

Draw Back of Gauss-Newton Method

- Convergence is not guaranteed.
- The procedure might progress gradually or fail to converge entirely if the initial estimation is distant from the minimum.
- Typically, the $J^T J$matrix is frequently either poorly conditioned or singular. To enhance and stabilize the Gauss-newton technique for non-linear predicaments, some type of regularization becomes necessary.

5.2. THEORY OF LEVENGBERG-MARQUARDT METHOD

According to the Gauss-Newton method

$$(J^T J)\delta = J^T (y_i - f(x_i, \beta)) \quad (1.48)$$

Applying damping terms to this, we get

$$(J^T J + \mu I)\delta_{lm} = g \; where \; g = J^T \big(y_i - f(x_i, \beta)\big) and \; \mu \geq 0. \quad (1.49)$$

Levenberg and Marquardt proposed employing a damped Gauss-Newton approach. The approach of adjusting the diagonal components of $J^T J$ is termed damping, and μ is denoted as the damping parameters.

The damping factor produces various impacts:

1) For every μ>0, the coefficient matrix is positive definite, guaranteeing thatδ_{lm}constitutes a downward direction.

2) For high values of μ we obtain

$$\delta_{lm} \cong \frac{1}{\mu} g \quad (1.50)$$

i.e., a brief movement in the most direct descent path. This is advantageous when the current iteration is distant from the solution.

3) when μ is exceedingly diminutive, $\delta_{lm} \cong \delta_{gn}$, which presents a beneficialadvancement during the concluding phases iteration, particularly when β approachesβ^*, where β^*represents the actual value.

Consequently, the damping parameter impacts both the direction and magnitude of the movement, prompting the development of a technique devoid of a dedicated line search. The selection of the initial μ-value should correspond to the magnitude of the elements within$A_0 = J(\beta_0)^T J(\beta_0)$, e.g. by letting

$$\mu_0 = \tau * max_i \left\{a_{ii}^{(0)}\right\} \quad (1.51)$$

Where τ is determined by the user. If the initial approximation is good to the true value of the parameter then $\tau = 10^{-6}$ otherwise $\tau = 10^{-3}$ or even 1. The adjustment is governed by the gain ratio.

$$\rho = \frac{F(\delta)-F(\delta+\delta_{lm})}{L(0)-L((\delta_{lm})}, \quad (1.52)$$

i.e., the ratio between the actual decrease and the predicted decrease in the function value as depicted in equation 1.51 where,

$L(0) - L(\delta_{lm}) = -2\delta_{lm}^T J^T Y\ \delta_{lm}^T J^T J\delta_{lm} as\ explained\ in$ equations given below from 1.52 to 1.56,

$$Y(\beta + \delta) \approx Y(\beta) + J(\beta)\delta \quad (1.53)$$

$$F(\beta + \delta) \approx L(\delta) = Y(\beta + \delta)^T Y(\beta + \delta) \quad (1.54)$$

$$= Y^T Y + 2\delta^T J^T Y + \delta^T J^T J\delta \quad (1.55)$$

$$= F(\beta) + 2\delta^T J^T Y + \delta^T J^T J\delta \quad (1.56)$$

$$F(\beta) = \sum_{i=1}^{m} (Y_i\,(\beta))^2 = \|Y(\beta)\|^2 = Y\beta^T Y(\beta) \quad (1.57)$$

Where $Y_i(\beta) = y_i - f(x_i, \beta) and\ f(x_i, \beta)$ is a fitting model

So if the value of ρ>0 then the updated damping factor μ is given by

$$\mu = \mu * max\left\{\frac{1}{3}, 1 - (2 * \rho - 1)^3\right\} \quad (1.58)$$

In the above equation if lies in the range of 0 to 0.5 then the updated damping factor μ will be equal to$1 - (2 * \rho - 1)^3$. If the value of ρ is greater than 0.5 then the updated value of the damping factor will be reduced by 1/3 of the previous value.

If the value of ρ is less than zero then the damping factor μ will be double the previous value.

A substantial ρ value signifies that $L(\delta_{lm})$ closely approximates $F(\beta + \delta_{lm})$, thus allowing for its reductionto align the subsequent Levenberg-Marquardt step with the Gauss-Newton direction. If ρ is diminutive (potentially even negative), then $L(\delta_{lm})$ serves as an inadequate approximation, prompting a doubling of μ to align more closely with the steepest descent path and diminish the stride length.

The termination conditions for the algorithm ought to acknowledge that at a global minimum, we have $F'(\beta^*) = 0$, allowing for the utilization of

$$\|g\|_\alpha \leq \varepsilon_1 \quad (1.59a)$$

Where $\varepsilon_1$represents a small, positive value, determined by the user. Another pertinent criterion involves halting if there's a minor alteration in δnamely,

$$\|\delta_{new} - \delta\| \leq \varepsilon_2(\|\delta\| + \varepsilon_2) \quad (1.59b)$$

This expression offers a gradual transition from a relative step size ε_2 when $\|\delta\|$ substantial absolute step size ε_2^2 if δapproaches 0. Ultimately, akin to all iterative procedures, a precaution against an endless loop is indispensable.

$$k \geq k_{max} \quad (1.59c)$$

Where ε_2 and k_{max} are chosen by the user.

6. STATE-OF-THE-ART

Whistlers refer to the low-frequency electromagnetic wave energy, typically right-circularly polarized, traversing the magnetic field within the ionosphere as well as the magnetosphere [76]. Within space research, a whistler has been specifically defined as an electromagnetic field produced by lightning that disperses as it passes through the magnetosphere and ionosphere. Sometimes referred to as "helicons," bounded whistlers are quasi-electromagnetic waves with a left- or right-hand polarization. Whistlers, on the other hand, are only electromagnetic in nature and only exhibit right-hand polarization [77]. Aigrain [78] introduced the term "helicon" in 1960 to characterize electromagnetic waves propagating within solid metal. Bowers et al. [79] were the first to observe helicon waves in metallic sodium and simultaneously examined their dispersion relation. Lehane and Thiemann [80] were the first researchers to experimentally investigate helicons in the toroidal ZETA fusion device. In their investigation of helicon wave propagation into non-uniform plasma, Blevin et al. [81] provided a qualitative explanation that clarified some of the differences in the middle of the uniform plasma theory for helicon waves and the experimental results of Lehane et al. [80]. Boswell et al. [82] pioneered the application of helicon waves in 1970 as a highly effective method for producing high-density plasma (~10^{19} m^{-3}). The increased interest in helicon plasma physics can be attributed to the efficient plasma production achieved through helicon waves. Plasma possessing high density and low electron (ion) temperature holds practical value as a viable source for plasma applications. Various applications benefit from the helicon source, encompassing industrial plasma processing [83, 84], pre-ionization [85, 86], current simulation for fusion systems [87–89], generation of negative ions [90, 91], and space plasma propulsion systems [92–95]. Moreover, helicon sources contribute significantly to diverse fundamental research areas, examples encompass research on dual strata, parametric deterioration instability, pressure-induced drift wave instability, and experiments with high beta. and the analysis of instability and turbulence in plasma confinement experiments. Researchers have considered a multitude of Collision and collision-less processes over the last three decades, aiming to understand their respective roles in the efficient plasma production associated with helicon waves. Chen [96] introduced the idea of Landau damping as an appropriate choice for energy transmission to the plasma. He described Landau damping as a Collisionless process where the wave power is conveyed to particles near the wave's phase velocity. Using RF-modulated emissions for Ar+ light to identify hot electrons, Molvik et al. [97] demonstrated the Landau damping associated with the wave. However, this interpretation was subsequently disproved since the experiment's fast electron count was insufficient [98]. A comparative study of various research papers has been presented in Table 4.

Table 4: Comparative assessment of matching techniques: advantages and applications.

Types of Antenna	Frequency	Favored Methodologies/Techniques	Findings	Advantages	Applications	Referen
Arch antenna	2.45 GHz	1. Low hybrid current drive (LHCD) 2. Left and right rectangular waveguides	i. 27 antenna elements ii. Refraction parallel index= 4.3 iii. Reflection coefficient (S_{11})= -12Db iv. Transition coefficient(S_{21})= 35 kA	i. Simple feeding ii. Low energy loss iii. High directivity	EXL-50 spherical Tokamak	99.
Spiral antenna	35-60 MHz	Electron cyclotron resonance method	i. Electron density $n_e \cong 10^{16} m^{-3}$ ii. RF power= 500W iii. RF plasma density 10^{16}V/m iv. Electron density of T_e=2-6 eV v. Electric field of the order of 10^6V/m vi. Toroidal magnetic field= 3T	i. The acquired density proves to be satisfactory for achieving low loop voltage breakdown in SST-1. ii. A notable quantity of charged particles are retained within the surrounding magnetic field throughout the breakdown phase.	Steady-state superconducting tokamak (SST-1)	100.
4-turn flat spiral antenna	13.56 MHz	Helicon wave plasma discharge	i. Magnetic field= 2T ii. Electron density =$10^{12}m^{-3}$ iii. RF power= 1500W iv. Pressure= 1Pa v. Helicon wave plasma discharge vi. The density of helium plasma, approximately around $10^{12}cm^{-3}$was assessed using a Langmuir probe.	i. A rise in the toroidal magnetic field from 0.5 to 2T led to increased uniformity within the plasma.	Experimental advanced superconducting tokamak (EAST)	101.
Traveling wave antenna	15-201 MHz	Fast wave current drive technique	i. Sharp N_Z spectrum achieved ii. RF generator power is= 800kW at a frequency of 200MHz. iii. Electron temperature= 3KeV iv. Voltage standing wave ratio (VSWR)=1.35	i. Faraday shield was proposed for better antenna-plasma coupling. ii. The outer helical support is attractive, because of its compact and tight structure	JFT-2M	102.

			v. Reflected power is below 0.05%.			
Two strap antenna	25-70 MHz	ICRH system	i. Fed by 30Ω transmission line ii. Copper wires with a diameter of 0.5mm iii. Working frequency = 37 MHz iv. Antenna probe coupling coefficient = -54.4 dB v. Coupling coefficient= -84 dB vi. Improved antenna phasing accuracy.	i. To mitigate mutual coupling between two antenna straps, a specialized decoupling mechanism was created. ii. An impedance-matching system with three tuning points was created to address the issue of impedance mismatch. iii. The creation of a directional coupler enabled the measurement of both input and reflected ICRF power.	EAST tokamak	103.
ICRH antenna	40-70 MHz	ICRH system	i. Major radius= 1.75m ii. Minor radius= 0.40m iii. B_T = 3.50 T iv. I_P = 1.00 MA v. T_{pulse} = 1000s vi. Edge density = N_3= 5 × $10^{17}m^{-3}$	i. Through numerical simulations, it is demonstrated that an appropriately chosen layout for the optimum feed location is advantageous in rendering tunable capacitors insensitive to fluctuations in the antenna input impedance when ELMy plasmas occur.	EAST-RDL (resonant double loop)	104.
ICRF antenna	35MHz	ICRF wave coupling	i. Major radius=R= 1.88m ii. Minor radius=a=0.45m iii. Radial position of the limitor R_0=2.34m iv. I_P= 400~ 500Ka v. Toroidal magnetic field B=2.2~2.5T vi. Frequency=34MHz vii. Total ICRF power= 0.5~2MW iii. Parallel wave no.$\|k_{11}\|$= 13.64	i. Efficient methods for optimizing coupling efficiency are discussed in conjunction with the theoretical interpretation of the results.	EAST tokamak	105.

			ix. Cut off density= $n_{cutoff}=9\times10^{18}/m^3$			

7. CONCLUSIONS

The exploration of helical antennas and their impact on antenna-plasma coupling impedance in the context of ICRH for tokamak applications has revealed valuable insights into the intricacies of plasma heating mechanisms. The study has delved into the design considerations, performance characteristics, and challenges associated with spiral antennas, shedding light on their effectiveness in enhancing the efficiency of ICRH heating processes. The examination of antenna-plasma coupling impedance has offered a nuanced understanding of the complex interplay between the electromagnetic waves and the plasma medium within the tokamak environment. The state-of-the-art helicon plasmas show various techniques and the challenges of designing the parameters of various antennas to further improve their performance in tokamak scenarios. The non-linear least square technique has been also discussed in the study. Additionally, investigating novel materials and advanced technologies for antenna construction may open up new avenues for enhancing efficiency and reliability. Collaborative efforts between researchers in plasma physics, antenna engineering, and materials science will be crucial in advancing the field and overcoming existing challenges. The study serves as a foundation for future research endeavors, offering a roadmap for researchers and engineers to navigate as they strive to improve the efficacy of ICRH heating in tokamak devices. As we continue to unravel the complexities of plasma physics and antenna technologies, the prospects for achieving controlled nuclear fusion for energy production become increasingly promising.

8. LIST OF ABBREVATIONS

SST-1	Steady state Superconducting Tokamak-1
ICRH	Ion Cyclotron Resonance Heating
RF	RF Radio frequency
ECRH	Electron cyclotron resonance heating
NBI	Neutral-beam injection
EAST	Experimental advanced superconducting tokamak
KSTAR	Korea Superconducting Tokamak Advanced Research
JT-60	Japan Torus-60
ECCD	Electron cyclotron current drive
ST	Spherical tokamak

JET	Joint European Torus
IPR	Institute for plasma research
ASDEX	Axially Symmetric Divertor Experiment
PEC	Perfect electric conductor
PLT	Princeton Large Torus
PPPL	Princeton Plasma Physics Laboratory
ORL	Oak Ridge Laboratory
ITER	International Thermonuclear Experimental Reactor
LMA	Levenberg-Marquardt algorithm
DLS	Damped least-squares
GNA	Gauss-Newton algorithm

9. DECLARATIONS:

Availability of data and materials

All the related data provided in the article.

Competing Interests

The authors declare no conflicts of interest that could influence the objectivity and impartiality of the research.

Funding

This research did not receive external funding from any organization. The study was conducted independently without financial support from external sources.

Author's Contributions

DY have written original draft, resorces, methodology, and conceptualization. VS conducted literature review. MK provided expertise in the subject matter, revised the manuscript critically for important and intellectual content. VG has done the visualization and supervision of the manuscript.

Acknowledgments

The research simulations were performed using CST-MWS software at Banasthali Vidyapith. The authors extend their appreciation to the IPR team for providing the opportunity to gain insights into a different tokamak located at IPR.

REFERENCES

1. "Energy policy of India", En.wikipedia.org. [online] Available at: https://en.wikipedia.org/wiki/Energy_policy_of_India [Accessed 11th March 2017].
2. "Nuclear Fusion Basics", Iaea.org. [online] Available at: https://www.iaea.org/newscenter/news/nuclear-fusion-basics [Accessed 12 Sep. 2016].
3. High field, R., Jamieson, V., Calder, N., & Arnoux, R., Iter: A brief history of fusion. New Scientist, 2, 2009.
4. "Tokamak", En.wikipedia.org. [online] Available at: https://en.wikipedia.org/wiki/Tokamak [Accessed 2 Oct. 2016].
5. Bora, D., Kumar, S., Singh, R., Kulkarni, S. V., Mukherjee, A., Singh, J. P.,& Bhattacharya, D. S., "Ion cyclotron resonance heating system on Aditya", Sadhana, vol. 30, pp. 21-46, 2005.
6. Bora, D., Kumar, S., Singh, R., Sathyanarayana, K., Kulkarni, S. V., Mukherjee, A., & Tai, E., "Cyclotron resonance heating systems for SST-1", Nuclear Fusion, vol. 46(3), pp. S72, 2006.
7. Rathi, D., Singh, R., & Kulkarni, S. V., "Design, fabrication and testing of the pressurized co-axial directional coupler for high RF power measurements for SST-1 ICRH system", In 2008 International Conference on Recent Advances in Microwave Theory and Applications, pp. 590-592, 2008
8. Parihar, M. S., Rajnish, K., Joshi, R., Jadav, H. M., George, S., Singh, R.,& Kulkarni, S. V., "Testing and Optimization of Matching Response Time for the Real Time Feedback Controlled ICRH-Automatic Matching Network (AMN) System for SST-1", IPR Technical Report, IPR/TR-139/2007.
9. Joshi, R., Singh, M., Jadav, H. M., Purohit, D., George, S., Rajnish, K., &Icrh-Rf Group, "Automatic impedance matching network for ICRH-RF experiments on SST-1", In Journal of Physics: Conference Series, vol. 208, pp. 012015, 2010.
10. Pradhan, S., Khan, Z., Tanna, V. L., Sharma, A. N., Doshi, K. J., Prasad, U.,& Bora, D., "The first experiments in SST-1", Nuclear fusion, vol. 55(10), pp. 104009, 2015.
11. Mishra, S. K., Misra, S., & Sodha, M. S., "Charging and de-charging of dust particles in bulk region of a radio frequency discharge plasma", Physics of Plasmas, vol. 20(3), 2013.
12. Joshi, R., Singh, M., Jadav, H. M., Mishra, K., Singh, R., Kulkarni, S. V.,& ICRH-RF Group, "Online impedance matching system for ICRH-RF experiments on SST-1 tokamak",Fusion Engineering and Design, vol. 100, pp. 293-300, 2015.
13. Joshi, R., Jadav, H. M., Mali, A., & Kulkarni, S. V., "Integration of PLC based offline impedance matching system for ICRH experiments", In 2016 2nd International Conference on Contemporary Computing and Informatics (IC3I),pp. 564-567, 2016.
14. R. P. Yadav, Ph.D. thesis, Institute for Plasma Research (IPR), 2014.
15. England, A. C., "Electron cyclotron heating experiments in tokamaks and stellarators", IEEE Transactions on Plasma Science, vol. 12(2), pp. 124-133, 1984.
16. Goulding, R. H., Hoffman, D. J., Conner, D. L., Hammonds, C. J., Ping, J. L., Riemer, B. W.,& Yugo, J. J., "The ORNL fast-wave ICRF antenna for alcator C-MOD", In IEEE Thirteenth Symposium on Fusion Engineering, pp. 215-220, 1989.
17. Takase, Y., Golovato, S., Porkolab, M., Bajwa, K., Becker, H., & Caldwell, D., "Engineering design and analysis of the Alcator C-MOD two-strap ICRF antenna", In [Proceedings] The 14th IEEE/NPSS Symposium Fusion Engineering, pp. 118-121, 1991.
18. Parisot, M.Sc. thesis, Massachusetts Institute of Technology (MIT), 2004.
19. Lin, Y., Binus, A., &Wukitch, S. J., "Real-time fast ferrite ICRF tuning system on the Alcator C-Mod tokamak", Fusion Engineering and Design, vol. 84(1), pp. 33-37, 2009.

20. Lin, Y., Binus, A., Wukitch, S. J., Koert, P., Murray, R., & Pfeiffer, A., "ICRF antenna matching system with ferrite tuners for the Alcator C-Mod tokamak", In AIP Conference Proceedings, pp. 16-25, 2015.
21. Golovato, S. N., Beck, W., Bonoli, P., Fridberg, M., Porkolab, M., & Takase, Y., "Antennas for ICRF heating in the Alcator C-Mod tokamak", In 15th IEEE/NPSS Symposium, Fusion Engineering, pp. 1069-107, 1993.
22. Takase, Y., Golovato, S., Porkolab, M., Becker, H., Gwinn, D., Kochan, S.,& Pierce, N., "Alcator C-MOD ICRF antenna design and analysis", In IEEE Thirteenth Symposium on Fusion Engineering, pp. 211-214, 1989.
23. Hofmeister, F., Braun, F., & Wesner, F., "The RF system and matching procedure for ASDEX and ASDEX Upgrade", Fusion engineering and design, vol. 24(1-2), pp. 83-89, 1994.
24. Prechtl, M., Bobkov, V., Braun, F., Faugel, H., &Noterdaeme, J. M., "Theory on dynamic matching with adjustable capacitors for theICRF system of ASDEX Upgrade", Fusion Engineering and Design, vol. 84(7-11), pp. 1539-1543, 2009.
25. Noterdaeme, J. M., Bobkov, V. V., Bremond, S., Parisot, A., Monakhov, I., Beaumont, B.,& Nightingale, M., "Matching to ELMy plasmas in the ICRF domain", Fusion Engineering and Design, vol. 74(1-4), pp. 191-198, 2005.
26. Křivská, A., "Antenna Modelling for Ion Cyclotron Resonant heating of Tokamak Plasmas" (Doctoral dissertation, Czech Technical University), 2013.
27. Manheimer, W. M., "Electron cyclotron heating of tokamaks", Infrared and Millimeter Waves: Instrumentation, vol. 2, pp. 299, 2014.
28. Jacquinot, J., Anderson, R. J., Arbez, J., Bartlett, D., Beaumont, B., Behringer, K.,& Walker, C. I., "ICRF studies on JET", Plasma Physics and Controlled Fusion, vol. 28(1A), pp. 1-6, 1986.
29. Campbell, D. J., Start, D. F. H., Wesson, J. A., Bartlett, D. V., Bhatnagar, V. P., Bures, M.,& Tonetti, G., "Stabilization of sawteeth with additional heating in the JET tokamak", Physical review letters, vol. 60(21), pp. 2148, 1988.
30. Walton, R. C., Agarici, G., Amarante, G., Baity, W., Beaumont, B., Brémond, S.,& Contributors, J. E., "Mechanical design of the ICRH antenna for JET-EP", In Symposium on Fusion Engineering, vol. 19(1), pp. 103-106, 2002.
31. Mayoral, M. L., Monakhov, I., Walden, T., Bobkov, V. V., Blackman, T., Graham, M.,& JET-EFDA contributors, "Hybrid couplers on the JET ICRF system: commissioning and first results on ELMs", In AIP Conference Proceedings, vol. 933, pp. 143-146, 2007.
32. Durodié, F., Nightingale, M., Argouarch, A., Berger-By, G., Blackman, T., Caughman, J., & Zastrow, K. D., "Commissioning of the ITER-like ICRF antenna for JET", Fusion Engineering and Design, vol. 84(2-6), pp. 279-283, 2009.
33. Graham, M., Mayoral, M. L., Monakhov, I., Ongena, J., Blackman, T., Nightingale, M. P. S. & JET-EFDA contributors, "Implementation of load resilient ion cyclotron resonant frequency (ICRF) systems to couple high levels of ICRF power to ELMy H-mode plasmas in JET", Plasma Physics and Controlled Fusion, vol. 54(7), pp. 074011, 2012.
34. Monakhov, I., Graham, M., Blackman, T., Dowson, S., Durodie, F., Jacquet, P., & JET-EFDA Contributors, "Design and operations of a load-tolerant external conjugate-T matching system for the A2 ICRH antennas at JET", Nuclear Fusion, vol. 53(8), pp. 083013, 2013.
35. Hoffman, D. J., Baity, F. W., Bryan, W. E., Chen, G. L., Luk, K. H., Owens, T. L.,& Walls, J. C., "The design of high-power ICRF antennas for TFTR and Tore Supra", In AIP Conference Proceedings, vol. 159, pp. 302-305, 1987.

36. Vulliez, K., Argouarch, A., Bosia, G., Berger-By, G., Bremond, S., Colas, L.,& Tore Supra Team, "Validation of the load-resilient ion cyclotron resonance frequency antenna concept on Tore Supra plasma", Nuclear fusion, vol. 48(6), pp. 065007, 2008.
37. Vervier, M., Dumortier, P., Grine, S., Messiaen, A., & Van Wassenhove, G., "Tests and matching analysis of a load resilient ICRH antenna on TEXTOR", Fusion Engineering and Design, vol. 74(1-4), pp. 377-383, 2005.
38. Messiaen, A., Dumortier, P., Koch, R., Lamalle, P., Louche, F., Martini, J. L., &Vervier, M., "Realisation of a test facility for the ITER ICRH antenna plug-in by means of a mock-up with salted water load", Fusion Engineering and Design, vol. 74(1-4), pp. 367-375, 2005.
39. Lamalle, P. U., Messiaen, A. M., Dumortier, P., & Louche, F., "Recent developments in ICRF antenna modeling", Nuclear Fusion, vol. 46(4), pp. 432, 2006.
40. Messiaen, A., Vervier, M., Dumortier, P., Lamalle, P., & Louche, F., "Study of the ITER ICRH system with external matching by means of a mock-up loaded by a variable water load", Nuclear Fusion, vol. 46(7), pp. S514, 2006.
41. Dumortier, P., Lamalle, P., Leroy, N., Messiaen, A., &Vervier, M., "Tests of load resilient matching procedure for the ITER ICRH system on a mock-up and layout proposal", Fusion Engineering and Design, vol. 82(5-14), pp. 758-764, 2007.
42. Messiaen, A., Vervier, M., Dumortier, P., Grine, D., Lamalle, P. U., Durodié, F., &Weynants, R., "Preparing ITER ICRF: development and analysis of the load resilient matching systems based on antenna mock-up measurements", Nuclear Fusion, vol. 49(5), pp. 055004, 2009.
43. Dumortier, P., Louche, F., Messiaen, A., Tamain, P., &Vervier, M., "RF optimization of the ITER ICRF antenna plug including its broad banding by a service stub", Fusion Engineering and Design, vol. 84(2-6), pp. 707-711, 2009.
44. Beaumont, B., Gassmann, T., Kazarian, F., Lamalle, P., Mukherjee, A., Baruah, U., & Sartori, R., "ITER ICRF system: R&D progress and technical choices", In 2009 23rd IEEE/NPSS Symposium on Fusion Engineering, pp. 1-4, 2009.
45. Dumortier, P., & Messiaen, A. M., "ICRH antenna design and matching", Fusion Science and Technology, vol. 57(2T), pp. 230-238, 2010.
46. Messiaen, A., &Weynants, R., "ICRH antenna coupling physics and optimum plasma edge density profile", Application to ITER. Plasma Physics and Controlled Fusion, vol. 53(8), pp. 085020, 2011.
47. Grine, D., Messiaen, A., Vervier, M., Dumortier, P., & Koch, R., "Summary and results of the study of the hybrid matching option implementation of the ITER ICRH system", Fusion Engineering and Design, vol. 87(2), pp. 167-178, 2012.
48. Vervier, M., Messiaen, A., & Dumortier, P., "Technical optimization of the ITER ICRH decoupling and matching system", Fusion Engineering and Design, vol. 88(6-8), pp. 1030-1033, 2013.
49. Kim, H. J., Wang, S. J., Park, B. H., Kwak, J. G., Hillairet, J., & Choi, J. J., "RF design and tests on a broadband, high-power coaxial quadrature hybrid applicable to ITER ICRF transmission line system for load-resilient operations",Fusion Engineering and Design, vol. 96, pp. 498-502, 2015.
50. Jain, A., Yadav, R. P., & Kulkarni, S. V., "Design and development of 2 kW, 3 dB hybrid coupler for the prototype ion cyclotron resonance frequency (ICRF) system", International Journal of Microwave and Wireless Technologies, vol. 11(1), pp. 1-6, 2019.
51. Kim, H. J., Bae, Y. S., Yang, H. L., Kwak, J. G., Wang, S. J., Kim, B. K., & Choi, J. J., "Ultra-wideband coaxial hybrid coupler for load resilient ion cyclotron range of frequency heating at fusion plasmas", Applied Physics Letters, vol. 100(26), 2012.

52. Song, K., Mo, Y., Zhuge, C., & Fan, Y., "Ultra-wideband (UWB) power divider with filtering response using shorted-end coupled lines and open/short-circuit slotlines", AEU-International Journal of Electronics and Communications, vol. 67(6), pp. 536-539, 2013.
53. Kim, H. J., Wang, S. J., Park, B. H., Kwak, J. G., Hillairet, J., & Choi, J. J., "RF design and tests on a broadband, high-power coaxialquadrature hybrid applicable to ITER ICRF transmission line system for load-resilient operations", Fusion Engineering and Design, vol. 96, pp. 498-502, 2015.
54. Yadav, R. P., Kumar, S., &Kulkarani, S. V., "Design and development of 3 dB patch compensated tandem hybrid coupler", Review of Scientific Instruments, vol. 84(1), 2013.
55. Kumazawa, R., Mutoh, T., Seki, T., Sinpo, F., Nomura, G., Ido, T., & Zhao, Y., "Liquid stub tuner for ion cyclotron heating", Review of Scientific Instruments, vol. 70(6), pp. 2665-2673, 1999.
56. Staples, J., & Schenkel, T., "High-efficiency matching network for RF-driven ion sources", In PACS2001. Proceedings of the 2001 Particle Accelerator Conference (Cat. No. 01CH37268), vol. 3(1), pp. 2108-2110, 2001.
57. Chengming, Q., Yanping, Z., Yuzhou, M., Jiayi, D., Peng, W., Yaping, P., &Guochao, L., "Design of a new type of stub tuner in ICRF experiment", Plasma Science and Technology, vol. 5(3), pp. 1779, 2003.
58. Yaping, P., Lei, W., Yanping, Z., Chengmin, Q., Diye, X., Xu, D. & Seki, T., "Design and realization of liquid stub tuner control system", Plasma Science and Technology, vol. 6(6), pp. 2531, 2004.
59. Girard, A., Hitz, D., Melin, G., &Serebrennikov, K., "Electron cyclotron resonance plasmas and electron cyclotron resonance ion sources", Physics and technology. Review of Scientific Instruments, vol. 75(5), pp. 1381-1388, 2004.
60. Bora, D., Kumar, S., Singh, R., Kulkarni, S. V., Mukherjee, A., Singh, J. P. & George, V., "Ion cyclotron resonance heating system on Aditya", Sadhana, vol. 30(1), pp. 21-46, 2005.
61. Saito, K., Kumazawa, R., Takahashi, C., Yokota, M., Takeuchi, H., Mutoh, T. & Komori, A., "Real-time impedance matching system using liquid stub tuners in ICRF heating", Fusion Engineering and Design, vol. 81(23-24), pp. 2837-2842, 2006.
62. Bora, D., Kumar, S., Singh, R., Sathyanarayana, K., Kulkarni, S. V., Mukherjee, A. &Kushwah, M., "Cyclotron resonance heating systems for SST-1", Nuclear Fusion, vol. 46(3), pp. S72, 2006.
63. Bacelli, G., Ringwood, J., & Iordanov, P., "Impedance matching controller for an inductively coupled plasma chamber: L-type Matching Network Automatic Controller", 2007.
64. Lin, Y., Binus, A., &Wukitch, S. J., "Real-time fast ferrite ICRF tuning system on the Alcator C-Mod tokamak", Fusion Engineering and Design, vol. 84(1), pp.33-37, 2009.
65. Hemsworth, R., Decamps, H., Graceffa, J., Schunke, B., Tanaka, M., Dremel, M.& Inoue, T., "Status of the ITER heating neutral beam system", Nuclear Fusion, vol. 49(4), pp. 045006, 2009.
66. Singh, R., Dani, S., Kulkarni, S. V., & Icrh-Rf Group, "Liquid phase shifter for ICRH for long pulse operation at SST-1", In Journal of Physics: Conference Series, vol. 208(1), pp. 012018, 2010.
67. Dani, S., Singh, R., Kulkarni, S. V., &Icrh-Rf Group, "Design of multi limb phase shifter", In Journal of Physics: Conference Series, vol. 208(1), pp. 012032, 2010.
68. Rathi, D., Mishra, K., Joshi, R., Jadav, H. M., & Kulkarni, S. V., "Conceptual design of automation of ICRH vacuum system on Aditya Tokamak", In Journal of Physics: Conference Series, vol. 208, pp. 012019, 2010.
69. Mishra, K., Kulkarni, S. V., Rathi, D., Varia, A. D., Jadav, H. M., Parmar, K. M.,& Kumar, S., "Direct electron heating experiment on the Aditya tokamak using fast waves in the ion cyclotron resonance frequency range", Plasma Physics and Controlled Fusion, vol. 53(9), pp. 095011, 2011.

70. Faugel, H., Bobkov, V., Braun, F., Franke, T., Hartmann, D. A., Kircher, M. & Team, A. U., "An improved method to measure the antenna resistance and radiated power of ICRF-antennas using current probes", Fusion Engineering and Design, vol. 86(6-8), pp. 996-999, 2011.
71. Bansal, G., Gahlaut, A., Soni, J., Pandya, K., Parmar, K. G., Pandey, R. & Chakraborty, A., "Negative ion beam extraction in ROBIN", Fusion Engineering and Design, vol. 88(6-8), pp. 778-782, 2013.
72. Lin, Y., Binus, A., Wukitch, S. J., Koert, P., Murray, R., & Pfeiffer, A., "ICRF antenna matching systems with ferrite tuners for the Alcator C-Mod tokamak", Fusion Engineering and Design, vol. 100, pp. 239-248, 2015.
73. Singh R., V. Dixit, V. Gahlaut, J. Ghosh, P. Tripathi, H. Kachhawa, U. K. Goswami, & V.P. Anita, "Investigation of developed liquid stub tuner for high-power RF plasma experiments", IEEE Transactions on Plasma Science, vol. 99(1), pp. 1-6, 2024.
74. Yadav D., M. Kaushik, P. Tiwari, V. Gahlaut, R. Singh, " Computational analysis of two-arm resistively loaded spiral antenna for SST-1 Tokamak", In 2023 IEEE Microwaves, Antennas and Propagation Conference (MAPCON),pp. 1-4, 2024.
75. Raj Singh, Dhaval Patel, Vishwa Dadhaniya, "Determination of Magnitude and Phase of Reflection Coefficient for ICRH Transmission Line on ADITYA Using Least Square Technique", IPR Research Report, IPR/RR-560/2012, 2012.
76. Stenzel, R. L., "Whistler waves in space and laboratory plasmas", Journal of Geophysical Research: Space Physics, vol. 104(A7), pp. 14379-14395, 1999.
77. Chen, F. F., "Physics of helicon discharges", Physics of Plasmas, vol. 3(5), pp. 1783-1793, 1996.
78. Hirota, R., "Theory of a solid-state plasma waveguide in a transverse magnetic field", Journal of the Physical Society of Japan, vol. 19(7), pp. 1130-1134, 1964.
79. Bowers, R., Legendy, C., & Rose, F., "Oscillatory galvano magnetic effect in metallic sodium", Physical Review Letters, vol. 7(9), pp. 339, 1961.
80. Lehane, J. A., &Thonemann, P. C., "An experimental study of helicon wave propagation in a gaseous plasma", Proceedings of the Physical Society, vol. 85(2), pp. 301, 1965.
81. Blevin, H. A., & Christiansen, P. J., "Propagation of helicon waves in a non-uniform plasma", Aust. J. Phys, vol. 19(501), 1966.
82. Boswell, R. W., "Plasma production using a standing helicon wave", Physics Letters A, vol. 33(7), pp. 457-458, 1970.
83. Perry, A. J., Vender, D., & Boswell, R. W., "The application of the helicon source to plasma processing", Journal of Vacuum Science & Technology B: Microelectronics and Nanometer Structures Processing, Measurement, and Phenomena, vol. 9(2), pp. 310-317, 1991.
84. Boswell, R. W., & Henry, D., "Pulsed high rate plasma etching with variable Si/SiO2 selectivity and variable Si etch profiles", Applied Physics Letters, vol. 47(10), pp. 1095-1097, 1985.
85. Stubbers, R., Jurczyk, B., Rovey, J., Coventry, M., Alman, D., & Walker, M., "Compact toroid formation using an annular helicon preionization source", In 43rd AIAA/ASME/SAE/ASEE Joint Propulsion Conference & Exhibit, pp. 5307, 2007.
86. Masters, B. C., Gray, T. K., Ruzic, D. N., & Stubbers, R., "Magnetic and Thermal Characterization of An ELM Simulating Plasma (ESP) With Helicon Pre-Ionization", In 21st IEEE/NPS Symposium on Fusion Engineering SOFE 05, pp. 1-4, 2005.
87. Loewenhardt, P. K., Blackwell, B. D., Boswell, R. W., Conway, G. D., & Hamberger, S. M., "Plasma production in a toroidal heliac by helicon waves", Physical Review Letters, vol. 67(20), pp. 2792, 1991.

88. Prater, R., Moeller, C. P., Pinsker, R. I., Porkolab, M., Meneghini, O., &Vdovin, V. L., "Application of very high harmonic fast waves for off-axis current drive in the DIII-D and FNSF-AT tokamaks", Nuclear Fusion, vol. 54(8), pp. 083024, 2014.
89. Paul, M. K., & Bora, D., "Current drive by helicon waves", Journal of Applied Physics, vol. 105(1), 2009.
90. Wang, S. J., Kwak, J. G., Kim, C. B., & Kim, S. K., "Observation of enhanced negative hydrogen ion production in weakly magnetized RF plasma", Physics Letters A, vol. 313(4), pp. 278-283, 2003.
91. Santoso, J., Manoharan, R., O'Byrne, S., & Corr, C. S., "Negative hydrogen ion production in a helicon plasma source", Physics of Plasmas, vol. 22(9), 2015.
92. Takahashi, K., "Helicon-type radiofrequency plasma thrusters and magnetic plasma nozzles", Reviews of Modern Plasma Physics, vol. 3(1), pp. 3, 2019.
93. Charles, C., "Plasmas for spacecraft propulsion", Journal of Physics D: Applied Physics, vol. 42(16), pp. 163001, 2009.
94. Longmier, B. W., Bering, E. A., Carter, M. D., Cassady, L. D., Chancery, W. J., Díaz, F. R. C.,& Squire, J. P., "Ambipolar ion accelerationin an expanding magnetic nozzle", Plasma Sources Science and Technology, vol. 20(1),pp. 015007, 2011.
95. Takahashi, K., Charles, C., Boswell, R., & Ando, A., "Performance improvement of a permanent magnet helicon plasma thruster", Journal of Physics D: Applied Physics, vol. 46(35), pp. 352001, 2013.
96. Chen, F. F., "Plasma ionization by helicon waves", Plasma Physics and Controlled Fusion, vol. 33(4), pp. 339, 1991.
97. Molvik, A. W., Ellingboe, A. R., & Rognlien, T. D., "Hot-electron production and wave structure in a helicon plasma source", Physical Review Letters, vol. 79(2), pp. 233, 1997.
98. Chen, F. F., & Blackwell, D. D., "Upper limit to Landau damping in helicon discharges", Physical Review Letters, vol. 82(13), pp. 2677, 1999.
99. Wang, Y., Zhou, Q., Wang, Z., Ma, W., Liu, C., & Shan, J., "Development of an arch antenna for LHCD in a spherical tokamak", Nuclear Fusion, vol. 63(5), pp. 056016, 2023.
100. Basu, D., Raju, D., Singh, R., Mukherjee, A., Patel, M., Rathi, D., & Raval, D., "Development of a novel spiral antenna system for low loop voltage current start-up at the Steady State Superconducting Tokamak (SST-1)", Plasma Physics and Controlled Fusion, vol. 64(1), pp. 015004, 2021.
101. Jin, C. G., Yu, T., Zhao, Y., Bo, Y., Ye, C., Hu, J. S., & Li, J. G., "Helicon plasma discharge in a toroidal magnetic field of the tokamak", IEEE Transactions on Plasma Science, vol. 39(11), pp. 3103-3107, 2011.
102. Saigusa, M., Moriyama, S., Fujii, T., & Kimura, H., "New conceptual antenna with spiral structure and back Faraday shield for FWCD (fast wave current drive)", (No. JAERI-CONF--94-001), 1994.
103. Liu, L. N., Liang, Q. C., Yang, H., Zhang, X. J., Yuan, S., Mao, Y. Z., & Zhang, K., "Measurement of the ICRH antenna phasing using antenna strap probe based diagnostic system in EAST tokamak", Nuclear Engineering and Technology, vol. 54(10), pp. 3614-3619, 2022.
104. Du, D., Gong, X., Wang, Z., Yu, J., & Zheng, P., "Theoretical analysis of the ICRH antenna's impedance matching for ELMy plasmas on EAST", Journal of Plasma Physics, vol. 78(6), pp. 595-599, 2012.
105. Zhang, J. H., Zhang, X. J., Cheng, Y., Qin, C. M., Zhao, Y. P., Mao, Y. Z.,& Kasahara, H., "Experimental analysis of the ICRF waves coupling in EAST", Nuclear Fusion, vol. 57(6), pp. 066030, 2017.